An sEMG Signal-based Robotic Arm for Rehabilitation applying Fuzzy Logic

Ngoc-Khoat Nguyen
Faculty of Control and Automation, Electric Power University, Hanoi, Vietnam
khoatnn@epu.edu.vn (corresponding author)

Thi-Mai-Phuong Dao
Faculty of Electrical Engineering, Hanoi University of Industry, Hanoi, Vietnam
daophuong@haui.edu.vn

Tien-Dung Nguyen
Faculty of Control and Automation, Electric Power University, Hanoi, Vietnam
dungnt@epu.edu.vn

Duy-Trung Nguyen
Faculty of Control and Automation, Electric Power University, Hanoi, Vietnam
trungnd@epu.edu.vn

Huu-Thang Nguyen
Faculty of Electrical Engineering, Electronics and Refrigeration - Thanh Hoa College of Industry, Thanh Hoa, Vietnam
nguyenhuuthang1983@gmail.com

Van-Kien Nguyen
Faculty of Electrical Engineering, Hanoi University of Industry, Hanoi, Vietnam
nguyenvankien197197@gmail.com

Received: 26 February 2024 | Revised: 5 April 2024 | Accepted: 8 April 2024

 DOI: https://doi.org/10.48084/etasr.7146

ABSTRACT

The recent surge in biosignal-based control signifies a profound paradigm shift in biomedical engineering. This innovative approach has injected new life into control theory, ushering in advancements in human-body interaction and control. Surface Electromyography (sEMG) emerges as a pivotal biosignal, attracting considerable attention for its wide-ranging applications across medicine, science, and engineering, particularly in the domain of functional rehabilitation. This study delves into the use of sEMG signals for controlling a robotic arm, with the overarching aim of improving the quality of life for people with disabilities in Vietnam. Raw sEMG signals are acquired via appropriate sensors and subjected to a robust processing methodology involving analog-to-digital conversion, band-pass and low-pass filtering, and envelope detection. To demonstrate the efficacy of the processed sEMG signals, this study introduces a robotic arm model capable of mimicking intricate human finger movements. Employing a fuzzy logic control strategy, the robotic arm demonstrates successful operation in experimental trials, characterized by swift response times, thereby positioning it as a valuable assistive device for people with disabilities. This investigation not only validates the feasibility of sEMG-based control for robotic arms, but also underscores its potential to significantly improve the lives of individuals with disabilities, a demographic that represents a substantial portion (approximately 8%) of the Vietnamese population.

Keywords-sEMG; digital signal processing; fuzzy logic control; robotic arm; rehabilitation

I. INTRODUCTION

Surface Electromyography (sEMG) offers a window into the world of muscle function. It works by capturing the electrical signals generated by muscle cells when they contract. These tiny electrical bursts, known as action potentials, are summed up by sEMG from a collection of muscle fibers beneath the skin in a localized area. sEMG has proven to be a valuable tool across various fields. In the realm of medicine, it helps to diagnose muscle, nerve, and joint disorders. Scientific research utilizes sEMG to delve deeper into muscle function, motor control, and rehabilitation strategies. Additionally, sEMG plays a crucial role in assistive technology, enabling control of devices such as robotic arms for people with disabilities.

The advantages of sEMG are undeniable. It is a non-invasive technique, requiring only electrodes placed on the skin for signal recording. Furthermore, sEMG is a safe and painless procedure, making it suitable for various settings, clinical or even at home. However, sEMG is not without limitations. The recorded signals can be susceptible to "noise" caused by factors, such as electrode placement, skin condition, and the intensity of muscle contraction. While sEMG offers valuable insights, it cannot provide detailed information on individual muscle cell activity. Data analysis from sEMG can also be complex and time-consuming. EMG signals refer to biological signals acquired by measuring voltage associated with the electrical activity generated in a muscle during contraction, providing an understanding into muscle nerve activity [1-2]. Techniques for gathering EMG signals encompass both invasive and non-invasive methods. Invasive Electromyography (iEMG) involves inserting a needle into the skin for measurement, while non-invasive approaches, known as sEMG, entail placing electrodes on the skin to collect data [3]. sEMG is preferred over its invasive counterpart due to its safety and simplicity. Surface electrodes come in two varieties: wet and dry. Wet electrodes, typically containing Ag/AgCl ions, offer superior quality and lower electrode-skin impedance but may cause skin irritation and degrade in quality over time as the gel dries. On the contrary, dry electrodes, despite having higher electrode-skin impedance, can capture more robust sEMG signals and are easier to use, eliminating the need for surface preparation procedures such as wet electrodes. Consequently, most studies on EMG sensors have opted for dry electrodes [4].

Finger movement relies on two opposing muscle groups in the forearm: flexors and extensors. Flexors, located on the front of the forearm, curl the fingers and the wrist. Examples include the flexor digitorum profundus and superficialis muscles. Extensors, situated on the back of the forearm, straighten the fingers and the wrist. Key extensor muscles include the extensor digitorum and the extensor digiti minimi. These groups collaborate to produce complex hand movements. When flexors contract, extensors relax, and vice versa. To capture the strongest EMG signals for finger control, electrodes are ideally placed on both the flexor and extensor muscle groups, preferably in the center for optimal signal strength.

II. BACKGROUND LITERATURE

Robots, especially robotic arms, have been studied for years and have been applied for many purposes [5-7]. In recent times, advancements in semiconductor technology have led to numerous successful efforts in designing EMG sensors that are progressively smaller, consume less energy and offer increased precision [8-13]. For example, in [11], an sEMG signal acquisition system with high frequency and low power consumption was developed. The results showed that the EMG signal samples obtained from this system were correlated by up to 99.5% with those from commercial systems while reducing power consumption by up to 92.72% and extending battery life by up to 9,057 times. In [12], an integrated sEMG sensor with a signal reading circuit, MCU, and BLE was presented for human-machine interface applications, achieving accuracy and stability exceeding 95%. This flexible, durable, and lightweight sensor, constructed on a multi-layer polyimide-coated copper sheet, is suitable for various individuals and muscle groups. In [13], a high-stability capacitive EMG sensor was developed, specifically adapted to the Otto Bock standard prosthetic limb, offering comfort during wear and avoiding skin irritation.

Furthermore, many studies have explored various algorithms for hand gesture classification using sEMG signals, with popular choices including Artificial Neural Networks (ANN), Linear Discriminant Analysis (LDA), and Support Vector Machine (SVM). Among these, ANN has garnered significant attention due to its ability to learn from examples, tolerance to noise, and generalization abilities in high-dimensional input spaces [14-17]. In [15], a surface electromyography (sEMG) signal classification system was meticulously examined based on Deep Neural Networks (DNN). The results, focusing on eight gestures, demonstrated that the DNN-based system outperformed other classifiers (average accuracy of 98.88%), including SVM, kNN, Random Forest, and Decision Tree. In [16], Machine Learning (ML) was employed to process shoulder and upper limb muscle signals, enabling the recognition of motion patterns and real-time control of an upper arm exoskeleton. The results demonstrated high accuracy, particularly with the SVM algorithm achieving 96 ± 3.8% accuracy offline and 90 ± 9.1% accuracy online, showcasing the reliability of ML in pattern recognition and exoskeleton motion control. In [18], a real-time hand gesture recognition model was presented, employing sEMG with a feedforward ANN, attaining an average recognition rate of 98.7% and an average response time of 227.76 ms across 12 subjects, each performing five gestures. In [19], a complete artificial arm control system was proposed to employ EMG signals. This control system also utilized a CMOS fuzzy chip for pattern recognition to control the robotic arm. In [20], a robotic system was introduced to support remote wrist home rehabilitation as an IoT application. The proposed control solution employing EMG signals incorporated a cascade fuzzy-based decision system to indicate the patient's pain. In [21], a wearable exoskeleton arm was designed and controlled with different control methods to assist people with muscle disorders in their arms and support their treatment. In this work, the fuzzy logic algorithm was trained with the PID controller block using EMG control signals. An adaptive Fuzzy Sliding Mode Control approach for an Assist-as-Needed

(AAN) strategy to accomplish effective human-exoskeleton synergy was proposed in [22]. The results revealed that the state trajectory errors and input torque were bounded within $\pm 5 \times 10^{-2}$ rad and ±5 Nm, respectively. An innovative approach to improve the efficiency and adaptability of upper limb exoskeleton robot-assisted rehabilitation was proposed in [23]. This approach involved the development of an Optimized Stimulation Control System (OSCS) in conjunction with fuzzy logic-based pain detection. In [24], an optimal fuzzy logic-based control strategy was proposed for a lower limb exoskeleton application. The control parameters for the proposed control approach were obtained by a recently developed optimization technique, called the Dragon Fly Algorithm (DFA). In these studies, sEMG signals were used together with intelligent control strategies, such as fuzzy logic inference, for rehabilitation. Although some studies might not employ sEMG, intelligent controllers still achieved good control performances. This idea inspired this study to integrate sEMG signals and a fuzzy logic control strategy to design and control a robotic arm model for rehabilitation, especially for Vietnamese people with disabilities.

III. PROCEDURE TO DESIGN AN SEMG SIGNAL-BASED ROBOTIC ARM

A. System Diagram

Before designing a real robotic arm, it is necessary to provide a diagram that represents the entire system. Figure 1 displays the main blocks of the proposed system. This system uses three sEMG sensors to collect the meaningful muscle activities to control the robotic arm. These sEMG sensors are classified into Gravity Analog EMG Sensors, developed in collaboration between DFRobot and OYMotion. They comprise two main elements: a module housing electrodes and another module integrating filtering and amplification circuits. Each of these sEMG sensors magnifies sEMG signals by 1000 times and mitigates noise via a differential input and comparable filtering circuit. The amplified sEMG signals are then sampled deploying a 10-bit Analog-to-Digital Converter (ADC) through the MCU's analog input. The signals collected from three sEMG sensors are transmitted to a microcontroller, as portrayed in Figure 1. Such a microcontroller is an integrated circuit designed to govern a specific operation in an embedded system. This component is responsible for processing sEMG signals received from the sensor, transmitting processed signals to the computer, and concurrently accepting control signals from the computer to regulate finger gestures, aligning with the operation of five servo motors. The power sources of the whole control system are a 5V battery for sensors and microcontrollers and a 12V battery for these 5 servo motors. The whole system is observed and controlled by a supervisory component, typically a PC or a laptop. Figure 2 depicts a simplified process for acquiring and processing sEMG signals. Raw sEMG outputs require further processing before they become suitable control signals for the robotic arm.

B. sEMG Signal Processing

The surface EMG sensor operates much like a Gravity sensor but with a remarkable ability to amplify weak muscle signals by a factor of 1000 times. This is made possible through a clever setup involving a combination of a differential input and a filtering circuit. These components work together to significantly reduce background noise. The sensor then produces an analog voltage signal ranging from 0 to 3.0 V, indicating the strength of muscle contractions.

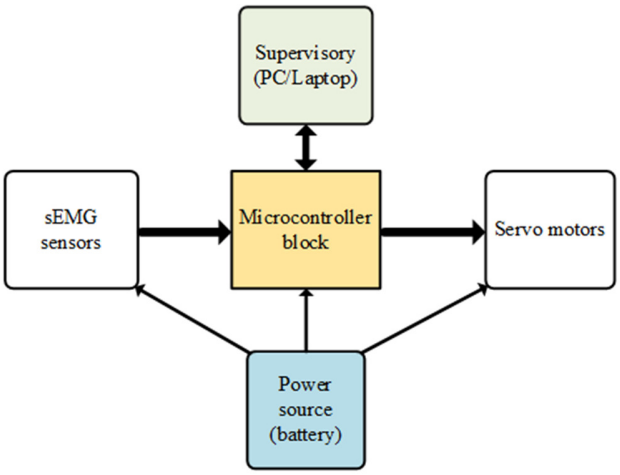

Fig. 1. A block diagram representing the whole control system.

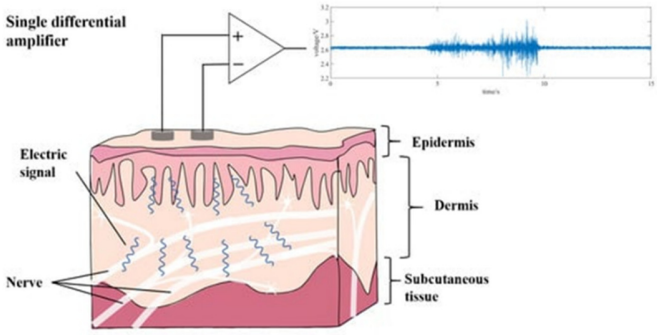

Fig. 2. An illustration of the surface EMG signal collection.

Figure 3 illustrates a step-by-step procedure to process the sEMG signals, which consists of the following stages:

1. Collect raw sEMG signals from the three sensors. This is the first step and should be implemented as carefully as possible.
2. Perform the Analog-to-Digital process. Analog signals collected from the sensors should be converted into digital counterparts to be easily used in signal processing. In this work, a digital format utilizing the microcontroller's 10-bit ADC, capturing data at a rapid rate of 1000 samples per second is employed. Once digitized, the signal undergoes further refinement through a high-pass filter, which effectively eliminates any additional unwanted noise.
3. Perform the digital signal processing. This phase typically includes three substeps to obtain the meaningful sEMG signals that can be used for the control goal. An envelope detection algorithm is applied to distill the essential information from the signal. This process extracts the core

data, resulting in a final processed output, as observed in Figure 3. In simple terms, digital filters act as gatekeepers of electrical signals. They sift through the data, removing undesirable noise and highlighting the elements that are of this study's interest. This is achieved through mathematical manipulations of the digital data. There are primarily two types of digital filters: Infinite Impulse Response (IIR) and Finite Impulse Response (FIR). The FIR filter is a fundamental tool in digital signal processing, renowned for its straightforward implementation and predictable behavior. Unlike its counterpart, the IIR filter, FIR operates by considering only past and present input data points, making it inherently stable and devoid of feedback loops. Its simplicity and stability make it particularly suitable for applications where precise control over frequency response and phase characteristics is paramount. By applying a finite number of coefficients to the input samples, the FIR filter effectively attenuates unwanted frequencies while preserving desired signal components. This versatility and reliability render FIR filters indispensable in a wide array of applications, from audio processing to telecommunications. The overarching mathematical formula of an FIR is expressed in:

$$y(n) = b_0x[n] + b_1x[n-1] + b_2x[n-2] + \ldots + b_Nx[N] \quad (1)$$

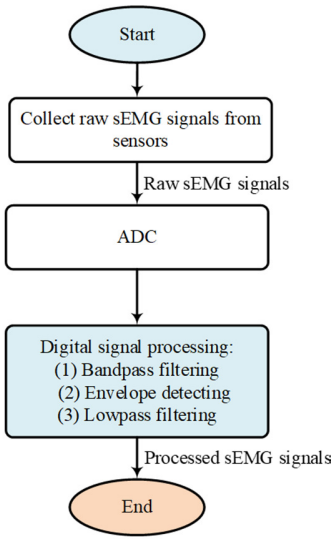

Fig. 3. A typical flow chart for processing sEMG signals.

In contrast to FIR filters, IIR filters exhibit a unique characteristic: feedback. This feedback mechanism allows IIR filters to consider both past and present input data, making them capable of achieving sharper roll-off characteristics and more compact filter designs compared to their FIR counterparts. However, this feedback also introduces challenges, such as potential instability due to the recursive nature of the filter. Despite this, IIR filters find extensive use in various applications, including audio equalization, biomedical signal processing, and control systems, where their efficiency and adaptability are valued. A typical expression of the IIR filter is given by:

$$\sum_{m=0}^{M} a_m y[n-m] = \sum_{k=0}^{N} b_k[n-k] \quad (2)$$

It is noted that a digital filter can take the form of either an IIR or an FIR filter. The key advantage of IIR filters over FIR filters lies in their ability to meet specific technical requirements using a considerably lower filter order compared to their FIR counterparts. Due to these benefits, this study used IIR filters to process EMG signals. One common approach to designing IIR filters involves initially designing an analogous filter and then converting it into a digital equivalent one. Various types of analogous low-pass filters, including Butterworth, Chebyshev, and Elliptic filters, offer differing intensity and phase responses. Extending this design to filters beyond low-pass involves frequency transformation techniques, yielding high-pass, band-pass, or band-stop filters corresponding to the prototype low-pass filter. Following this, the analogous IIR filter is transformed into a digital filter adopting methods, such as impulse invariant, backward difference, or bilinear z-transform. This study used a second-order IIR Butterworth digital filter for EMG signal filtration. The low-cut frequency was set at 50Hz to eliminate low-frequency noise, and the high-cut frequency at 150Hz to mitigate high-frequency noise. A sampling frequency of 1 KHz was chosen, based on [14, 15], which suggests that a frequency between 400 and 500Hz is adequate for an EMG signal measurement. The transfer function of the filter is:

$$H(z) = \frac{Y(z)}{X(z)} = \frac{0.106z - 0.212z^{-1} + 0.106z^{-2}}{1 - 0.754z^{-1} - 0.392z^{-2} + 0.754z^{-3} + 1.006z^{-4}} \quad (3)$$

The ultimate low-pass filter refines the output signal derived from the envelope detector algorithm, ensuring a smoother and more accurate representation of the underlying muscle activity. A specific digital low-pass filter was designed for this task. This first-order IIR filter operates with a cut-off frequency of 10 Hz and a sampling frequency of 1 KHz. It strategically attenuates high-frequency components beyond the cut-off threshold while preserving the essential characteristics of the EMG signal within the desired frequency range. Equation (4) elucidates the transfer function, which delineates the filter's behavior and its role in enhancing the fidelity of the processed EMG signal for subsequent analysis and interpretation.

$$G_{LP}[z] = \frac{Y[z]}{X[z]} = \frac{b[0]}{a[0] + a[1]z - 1} \quad (4)$$

The equation uses z to represent the input signal and $Y[z]$ for the output. The filter is designed with two parameters: a and b. These are set to specific values to account for the delay caused by the filter. The values of a and b are determined based on the desired time constant (T) and the filter's cut-off frequency (f_c) as given in (5) and (6):

$$T = \frac{c\Delta t}{1-c} = \frac{1}{2\pi f_c} \quad (5)$$

$$c = \frac{1}{1 + \frac{\Delta t}{T}} = \frac{1}{1 + 2\pi f_c \Delta t} \quad (6)$$

This step-by-step process for processing sEMG signals makes them suitable for controlling a robotic arm, as long as a proper control strategy is implemented. This study employs fuzzy logic for this task.

C. Fuzzy Logic-Based Control Strategy

Fuzzy logic is a powerful tool for handling ambiguity and uncertainty in data. In the context of sEMG signal classification, it can be used to identify muscle activity states based on features extracted from the EMG signal. This approach enables an accurate determination of muscle activity levels while also addressing the inherent uncertainty and variability of EMG data. The pre-processing of EMG signals is an essential step in signal analysis and evaluation, helping to extract important features and reduce noise. Several major indices should be put into service to evaluate the quality of the sEMG signals in the preprocessing, such as Root Mean Square (RMS), Average Value Rectified (AVR), Maximum value (MAX), Variance (VAR), and Entropy (E). Figure 4 showcases the fuzzy logic structure applying these parameters for sEMG signal preprocessing. It is noted that there are three processing flows applied to the fuzzy logic model corresponding to the three sEMG channels employed in this work.

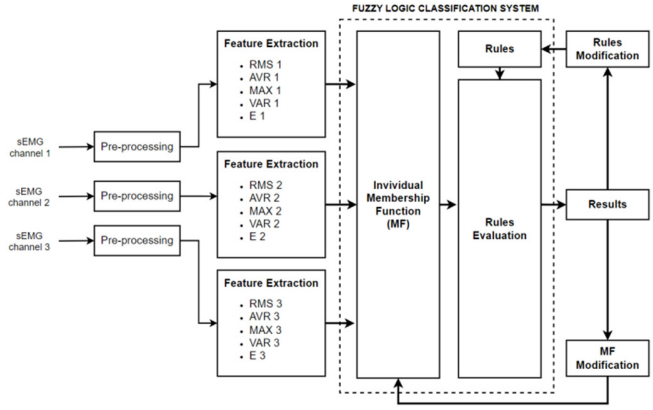

Fig. 4. Three control flows for the fuzzy logic methodology

TABLE I. FUZZY LOGIC RULES USED FOR THE CONTROL SYSTEM OF THE ROBOTIC ARM

No	sEMG channel 1	sEMG channel 2	sEMG channel 3	Result
1	BIG	BIG	BIG	Grasping the hand
2	MEDIUM	MEDIUM	MEDIUM	Bend the middle finger
3	BIG	MEDIUM	SMALL	Bend the ring finger
4	SMALL	BIG	MEDIUM	Bend the index finger
5	MEDIUM	MEDIUM	SMALL	Bend the little finger
6	SMALL	MEDIUM	BIG	Bend the thumb
7	SMALL	SMALL	SMALL	Blur the hand

In fuzzy logic-based EMG signal classification, fuzzy rules play a critical role in mapping EMG signal features to muscle activity states. These rules are constructed based on the expertise and experience of domain specialists in areas, such as kinesiology and biomechanics. Unlike traditional logic where variables are true or false, fuzzy logic allows for degrees of truth between 0 (completely false) and 1 (completely true). This flexibility is crucial when dealing with biological signals, like EMG, which exhibit inherent variability and uncertainty. The fuzzy rules capture imperfectly precise relationships between the extracted EMG features (e.g., amplitude, mean frequency) and the corresponding muscle activity states (e.g., rest, contraction, fatigue). These rules are typically expressed in an "if-then" format, namely "if the signal amplitude is high and the mean frequency is low, then the muscle activity is likely in a contraction state." Table I represents a specific set of fuzzy logic rules employed for this study, demonstrating how these rules translate the characteristics of the EMG signal into interpretable muscle activity states.

IV. EXPERIMENTS AND RESULTS

This study investigates the biomechanical characteristics of the human hand, involving bones and joints, to create a robot hand model. Simultaneously, some constraints of the robot hand are applied to simplify the motion model without significantly reducing its functionalities. The human hand comprises 27 bones, including 8 carpal bones, 5 metacarpal bones, and 14 phalangeal bones. The phalangeal bones (except for the thumb) consist of 3 phalanxes: proximal, middle, and distal. The thumb has only 2 phalanges: proximal and distal. These bones are connected through joints, allowing flexible movements from gripping to performing detailed activities. The distal phalanx and intermediate phalanx are connected by a DIP hinge joint (one degree of freedom). The intermediate phalanx is connected to the proximal phalanx by a PIP hinge joint (one degree of freedom). The proximal phalanx is connected to the metacarpal bone by an MCP ball joint (three degrees of freedom). The metacarpal bone is connected to the carpal bone by a CMC joint (six degrees of freedom).

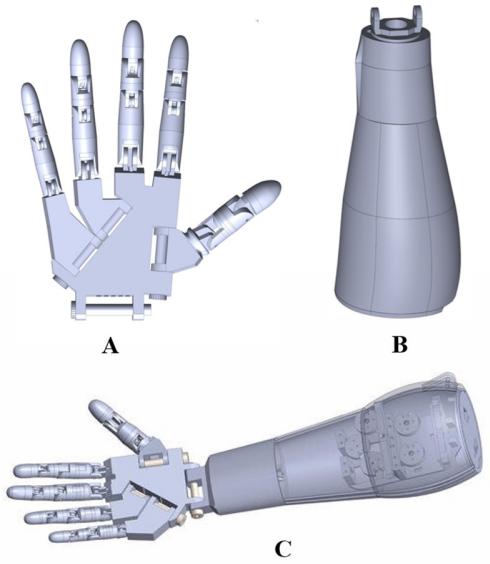

Fig. 5. The design of a 3D – robotic arm (InMoov): A: Robot hand; B: Robot arm; C: Entire robotic arm

In [25], some limitations of the human hand were presented. Specifically, each finger has a limited range of motion due to the mechanical constraints of hand anatomy. For example, the range of motion of the DIP joint is from 0 to 90°. In each finger, the DIP and the PIP joints always move

together. Therefore, to simplify the robot hand model, some joints in the robot hand design are modified compared to those in the human hand. The MCP joints in the index and little fingers for flexion-extension movements have a narrow range from -15° to 15°, and they are rarely involved in activities. Thus, these joints will be limited to one degree of freedom hinge joints. Figure 5 illustrates the mechanical model detail of the robot hand. With this design, each finger will have 3 hinge joints with rotation angles: θ_{DIP}, θ_{PIP}, and θ_{MCP}. θ_{DIP} is the rotation angle of the DIP joint, θ_{PIP} is the rotation angle of the PIP joint, and θ_{MCP} is the rotation angle of the MCP joint. Table II exhibits the rotation angle values of the robot hand joints.

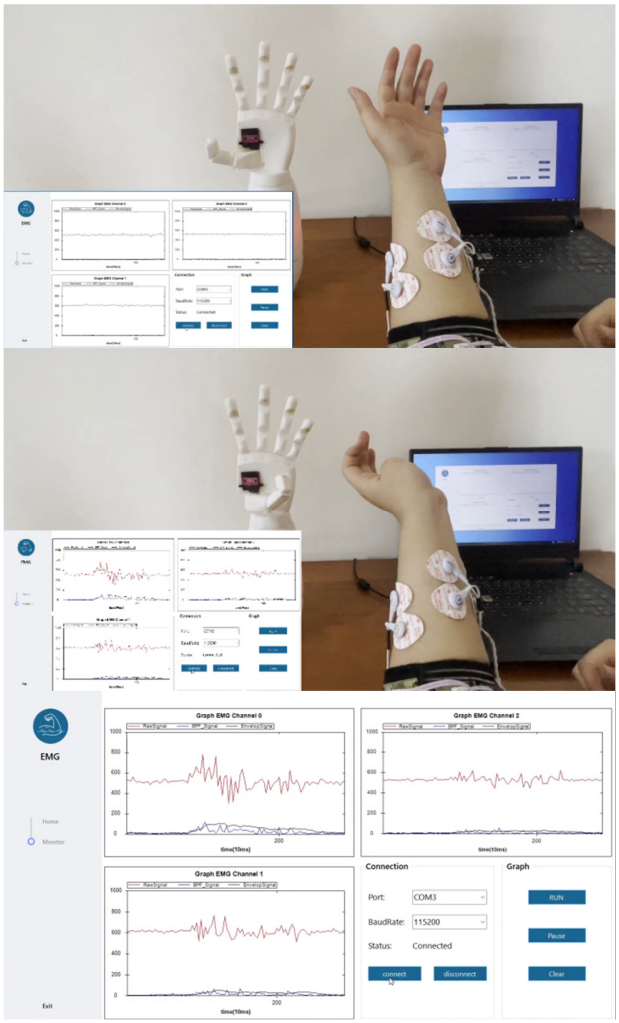

Fig. 6. The experimental results on the robotic arm model applied sEMG signals - thumb control: (a) Relax the hand, (b) Curl the thumb, and (c) waveform graphs.

This study used the open-source design of the InMoov robotic hand. With its 3D-printed structure (Figure 5), this hand is not only aesthetically pleasing, but also capable of mimicking natural hand movements. InMoov is not just limited to being a sophisticated robot product, but is also an open-source project, encouraging community involvement in its development and customization. The sEMG signal-controlled system makes it an excellent tool for learning and research in the field of assistive robotics. This study deploys three surface EMG sensors to record muscle activity in the arm. Sensor 1 specifically targets the index finger's movement, sensor 2 focuses on the combined activity of the middle and index fingers, and sensor 3 monitors thumb mobility. During periods of finger muscle relaxation, the raw sEMG signals acquired from the three sensors exhibit slight oscillations around the reference voltage threshold of 1.5 V. This oscillation frequency remains below the high-cut frequency of the digital high-pass filter, resulting in signal attenuation. Consequently, both the output signals from the bandpass filter and the envelope signals register zero values.

TABLE II. ANGLES OF MOVEMENT OF FINGER JOINTS

	θ_{DIP}	θ_{PIP}	θ_{MCP}
Thumb	-30° ÷ 90°	0° ÷ 90°	−10° ÷ 40°
Index	-30° ÷ 90°	0° ÷ 90°	−10° ÷ 20°
Middle	-30° ÷ 90°	0° ÷ 90°	−15° ÷ 15°
Ring	-30° ÷ 90°	0° ÷ 90°	−20° ÷ 10°
Little	-10° ÷ 30°	0° ÷ 90°	−10° ÷ 100°

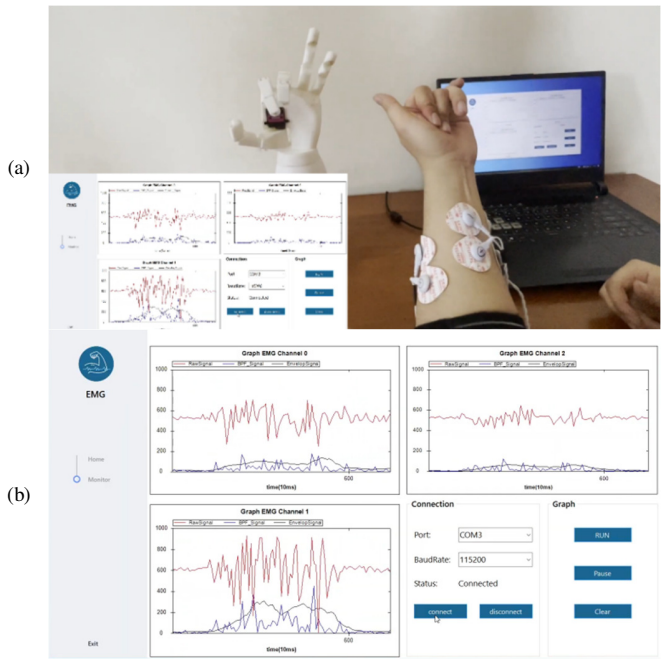

Fig. 7. The experimental results on the robotic arm model applied sEMG signals - controlling the index and middle fingers: (a) curl the fingers and (b) waveform graphs.

In contrast, when the fingers contract, the raw signals from the sEMG sensors display fluctuations with increased amplitude and frequency. The bandpass filter is employed to permit the passage of these signals. Through the application of an edge detection algorithm, an envelope signal is derived, reflecting the extent of muscle contraction, with its magnitude contingent on the level of contraction of the respective muscle. Figures 6-9 provide visual representations of the EMG signal activities captured during the execution of various basic motor tasks. The distinct patterns observed in these channels offer valuable insight into the muscle activation patterns associated with specific movements.

(a)

(b)

Fig. 8. Experimental results on the robotic arm model applied sEMG signals - controlling the pinky and ring fingers: (a) curl the fingers and (b) waveform graphs.

(a)

(b)

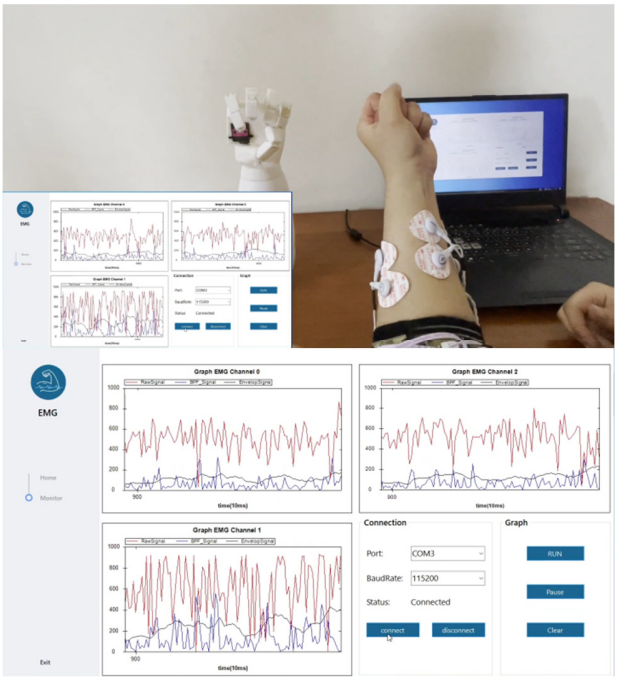

Fig. 9. Experimental results on the robotic arm model applied sEMG signals - hand grasp control: (a) hold the hand and (b) waveform graphs.

By analyzing these EMG signals, the effectiveness of the control strategy in translating human intention into corresponding robotic actions can be confirmed. The successful decoding of these signals empowers the robotic arm to mimic the user's movements with precision, paving the way for a more intuitive and natural human-machine interface. From this point of view, it is very meaningful for disabled people in rehabilitation.

V. CONCLUSIONS AND FUTURE WORK

This study meticulously focused on the efficient acquisition and processing of sEMG signals. These processed signals are then utilized to collaborate with a fuzzy logic model to control a sophisticated robotic arm model capable of replicating intricate human finger movements. The successful experimental results validate the stability and effectiveness of the model in translating human intention into precise robotic actions. Building upon this foundation, future endeavors will strive to enhance the robotic arm's functionalities. This includes incorporating wrist rotation, forearm flexion, and extension, allowing for a wider range of natural and coordinated movements. Furthermore, the research team plans to integrate advanced control algorithms in addition to the proposed fuzzy logic-based control strategy, such as ANNs. This will enable the robotic arm to seamlessly execute a diverse repertoire of movements, mimicking the dexterity and adaptability of the human hand. Notably, the modular design prioritizes future commercialization and widespread adoption. This focus is particularly relevant in emerging economies like that of Vietnam, where such advances can have a significant impact. By expanding the robotic arm's capabilities, the project contributes to a broader mission: fostering automation technologies and propelling economic development in regions poised to benefit greatly from these innovations. Ultimately, this study has the potential to not only improve the lives of people with disabilities, but also revolutionize various industries, paving the way for a more automated and efficient future.

APPENDIX

PARAMETERS OF THE MAIN COMPONENTS USED TO DESIGN THE EXPERIMENTAL ROBOT MODEL

No	Component	Specifications
1	Gravity Analog EMG	Supply voltage: + 3.3 V ~ 5.5 V Supply current: >20 mA Operating voltage: +3.0 V Detection range: +/- 1.5 mV Output voltage: 0 ~ 3.0 V Reference voltage: +1.5 V Gain: ×1000 Effective spectrum range: 20 ~ 500 Hz
2	MG996R Servo Motor	Motor type: DC motor servo Operating range: 0-180° Operating voltage: 4.8 ~ 7.2 VDC Running current: 500 ~ 900 mA (6V) Stall current: 2.5 A (6V) Stall torque: 9.4 kgf·cm (4.8 V), 11 kgf·cm (6 V) Operating speed: 0.17 s/60º (4.8 V), 0.14 s/60º (6V) Dead band width: 5 µs Weight: 55 g Dimension: 40.7 × 19.7 × 42.9 mm approx Temperature range: 0 ~ 55°C
3	ATMEGA32U4-MU	CPU family: AVR RISC Core size: 8-bit Program memory Size: 32 KB RAM: 2560 B Data EEPROM: 1024 B Frequency: 8 MHz (2.7 V), 16 MHz (4.5 V) Number of Terminations: 44

		Number of I/Os: 26 Operating voltage (V): 5.5 (Max), 2.7 (Min) Supply current-max: 15 mA Max ADC Resolution: 10 bits Number of ADC channels: 12 Number of PWM channels: 8 Number of timers/counters: 5 Number of USB channels: 1 Interface: I2C, SPI, UART/USART, USB Temperature range: -40 ~ 85°C

REFERENCES

[1] M. B. I. Reaz, M. S. Hussain, and F. Mohd-Yasin, "Techniques of EMG signal analysis: detection, processing, classification and applications," *Biological Procedures Online*, vol. 8, no. 1, pp. 11–35, Dec. 2006, https://doi.org/10.1251/bpo115.

[2] S. Kang, H. Kim, C. Park, Y. Sim, S. Lee, and Y. Jung, "sEMG-Based Hand Gesture Recognition Using Binarized Neural Network," *Sensors*, vol. 23, no. 3, Jan. 2023, Art. no. 1436, https://doi.org/10.3390/s23031436.

[3] A. Prakash, S. Sharma, and N. Sharma, "A compact-sized surface EMG sensor for myoelectric hand prosthesis," *Biomedical Engineering Letters*, vol. 9, no. 4, pp. 467–479, Nov. 2019, https://doi.org/10.1007/s13534-019-00130-y.

[4] D. Brunelli, A. M. Tadesse, B. Vodermayer, M. Nowak, and C. Castellini, "Low-cost wearable multichannel surface EMG acquisition for prosthetic hand control," in *2015 6th International Workshop on Advances in Sensors and Interfaces (IWASI)*, Gallipoli, Italy, 2015, pp. 94–99, https://doi.org/10.1109/IWASI.2015.7184964.

[5] L. Zouari, S. Chtourou, M. B. Ayed, and S. A. Alshaya, "A Comparative Study of Computer-Aided Engineering Techniques for Robot Arm Applications," *Engineering, Technology & Applied Science Research*, vol. 10, no. 6, pp. 6526–6532, Dec. 2020, https://doi.org/10.48084/etasr.3885.

[6] J. Iqbal, "Modern Control Laws for an Articulated Robotic Arm: Modeling and Simulation," *Engineering, Technology & Applied Science Research*, vol. 9, no. 2, pp. 4057–4061, Apr. 2019, https://doi.org/10.48084/etasr.2598.

[7] S. Z. Ying, N. K. Al-Shammari, A. A. Faudzi, and Y. Sabzehmeidani, "Continuous Progressive Actuator Robot for Hand Rehabilitation," *Engineering, Technology & Applied Science Research*, vol. 10, no. 1, pp. 5276–5280, Feb. 2020, https://doi.org/10.48084/etasr.3212.

[8] S. Glowinski, S. Pecolt, A. Błażejewski, and B. Młyński, "Control of Brushless Direct-Current Motors Using Bioelectric EMG Signals," *Sensors*, vol. 22, no. 18, Jan. 2022, Art. no. 6829, https://doi.org/10.3390/s22186829.

[9] Y. D. Wu, S. J. Ruan, and Y. H. Lee, "An Ultra-Low Power Surface EMG Sensor for Wearable Biometric and Medical Applications," *Biosensors*, vol. 11, no. 11, Nov. 2021, Art. no. 411, https://doi.org/10.3390/bios11110411.

[10] M. S. Song, S. G. Kang, K. T. Lee, and J. Kim, "Wireless, Skin-Mountable EMG Sensor for Human–Machine Interface Application," *Micromachines*, vol. 10, no. 12, Dec. 2019, Art. no. 879, https://doi.org/10.3390/mi10120879.

[11] T. Roland, K. Wimberger, S. Amsuess, M. F. Russold, and W. Baumgartner, "An Insulated Flexible Sensor for Stable Electromyography Detection: Application to Prosthesis Control," *Sensors*, vol. 19, no. 4, 2019, https://doi.org/10.3390/s19040961.

[12] J. Yousefi and A. Hamilton-Wright, "Characterizing EMG data using machine-learning tools," *Computers in Biology and Medicine*, vol. 51, pp. 1–13, Aug. 2014, https://doi.org/10.1016/j.compbiomed.2014.04.018.

[13] A. K. Mukhopadhyay and S. Samui, "An experimental study on upper limb position invariant EMG signal classification based on deep neural network," *Biomedical Signal Processing and Control*, vol. 55, Jan. 2020, Art. no. 101669, https://doi.org/10.1016/j.bspc.2019.101669.

[14] Z. Zhang, K. Yang, J. Qian, and L. Zhang, "Real-Time Surface EMG Pattern Recognition for Hand Gestures Based on an Artificial Neural Network," *Sensors*, vol. 19, no. 14, Jan. 2019, Art. no. 3170, https://doi.org/10.3390/s19143170.

[15] C. Larivière, A. Delisle, and A. Plamondon, "The effect of sampling frequency on EMG measures of occupational mechanical exposure," *Journal of Electromyography and Kinesiology*, vol. 15, no. 2, pp. 200–209, Apr. 2005, https://doi.org/10.1016/j.jelekin.2004.08.009.

[16] B. Chen *et al.*, "Volitional control of upper-limb exoskeleton empowered by EMG sensors and machine learning computing," *Array*, vol. 17, Mar. 2023, Art. no. 100277, https://doi.org/10.1016/j.array.2023.100277.

[17] S. S. Bangaru, C. Wang, S. A. Busam, and F. Aghazadeh, "ANN-based automated scaffold builder activity recognition through wearable EMG and IMU sensors," *Automation in Construction*, vol. 126, Jun. 2021, Art. no. 103653, https://doi.org/10.1016/j.autcon.2021.103653.

[18] G. Li, Y. Li, Z. Zhang, Y. Geng, and R. Zhou, "Selection of sampling rate for EMG pattern recognition based prosthesis control," in *2010 Annual International Conference of the IEEE Engineering in Medicine and Biology*, Buenos Aires, Argentina, Aug. 2010, pp. 5058–5061, https://doi.org/10.1109/IEMBS.2010.5626224.

[19] M. Mokarram and A. Khoei, "Designing a fuzzy CMOS chip for controlling an artificial arm using electromyogram signals," *Microelectronics Journal*, vol. 112, Jun. 2021, Art. no. 105053, https://doi.org/10.1016/j.mejo.2021.105053.

[20] Y. Bouteraa, I. B. Abdallah, A. Ibrahim, and T. A. Ahanger, "Fuzzy logic-based connected robot for home rehabilitation," *Journal of Intelligent & Fuzzy Systems*, vol. 40, no. 3, pp. 4835–4850, Jan. 2021, https://doi.org/10.3233/JIFS-201671.

[21] Ç. Ersin and M. Yaz, "Implementation and Comparison of Wearable Exoskeleton Arm Design with Fuzzy Logic and Machine Learning Control," *Journal of Sensors*, vol. 2024, Apr. 2024, Art. no. e6808322, https://doi.org/10.1155/2024/6808322.

[22] P. Delgado, N. Gonzalez, and Y. Yihun, "Integration of sEMG-Based Learning and Adaptive Fuzzy Sliding Mode Control for an Exoskeleton Assist-as-Needed Support System," *Machines*, vol. 11, no. 7, 2023, https://doi.org/10.3390/machines11070671.

[23] I. B. Abdallah and Y. Bouteraa, "An Optimized Stimulation Control System for Upper Limb Exoskeleton Robot-Assisted Rehabilitation Using a Fuzzy Logic-Based Pain Detection Approach," *Sensors*, vol. 24, no. 4, 2024, https://doi.org/10.3390/s24041047.

[24] R. Sharma, P. Gaur, S. Bhatt, and D. Joshi, "Optimal fuzzy logic-based control strategy for lower limb rehabilitation exoskeleton," *Applied Soft Computing*, vol. 105, Jul. 2021, Art. no. 107226, https://doi.org/10.1016/j.asoc.2021.107226.

[25] J. Lin, Y. Wu, and T. S. Huang, "Modeling the constraints of human hand motion," in *Proceedings Workshop on Human Motion*, Dec. 2000, pp. 121–126, https://doi.org/10.1109/HUMO.2000.897381.